

MPC-based Pedestrian Routing for Congestion Balancing

Menner, Marcel; Di Cairano, Stefano; Hamada, Masaki; Gushima, Kota

TR2023-099 August 18, 2023

Abstract

This paper presents a model predictive control (MPC)-based algorithm for guiding/routing pedestrians to balance congestion levels in crowded places such as train stations. The proposed algorithm uses arrow displays at junctions, whose guidance direction and display intensity are computed using MPC by leveraging pedestrian flow predictions. The MPC uses a congestion prediction model relating the display action to the percentage of pedestrians that are expected to change their intended walking direction, i.e., the percentage of pedestrians that are being re-routed. Simulation results show that the congestion imbalance can be reduced significantly using the proposed algorithm.

IEEE Conference on Control Technology and Applications (CCTA) 2023

MPC-based Pedestrian Routing for Congestion Balancing

Marcel Menner, Stefano Di Cairano, Masaki Hamada, and Kota Gushima

Abstract—This paper presents a model predictive control (MPC)-based algorithm for guiding/routing pedestrians to balance congestion levels in crowded places such as train stations. The proposed algorithm uses arrow displays at junctions, whose guidance direction and display intensity are computed using MPC by leveraging pedestrian flow predictions. The MPC uses a congestion prediction model relating the display action to the percentage of pedestrians that are expected to change their intended walking direction, i.e., the percentage of pedestrians that are being re-routed. Simulation results show that the congestion imbalance can be reduced significantly using the proposed algorithm.

I. INTRODUCTION

Crowd management is an important aspect of ensuring safety in large gatherings and crowded places such as train stations. Further, balanced congestion levels across different walkways can increase the average pedestrian walking speed and keeps traffic flowing efficiently. Balancing congestion levels in train stations is particularly important as an imbalance in congestion levels at the platform can reduce people throughput, because of varying boarding times at different parts of the train and also translate in imbalance in the train cars' load. Conventionally, pedestrians traversing a train station are not aware of congestion levels in different areas of the train station or at the different segments of a platform. Thus, guiding pedestrians toward less crowded parts of the platform and/or less crowded walkways can increase boarding efficiency and people throughput.

This paper presents a technology that uses an arrow display at a junction to guide pedestrians toward less crowded areas. The arrow display comprises of a guidance direction and an intensity level of the signal, where the latter relates to how prominent the arrow is displayed. We compute such parameters of the display using model predictive control (MPC). The MPC uses pedestrian flow predictions and to balance congestion levels in public infrastructure such as train stations. Fig. 1 illustrates a scenario at a train station, whose platform can be reached through two escalators. Here, we utilize the proposed algorithm to display an arrow in the direction of either of the two escalators to balance congestion at the platform. The MPC uses a congestion prediction model, whose states relate to the number of pedestrians in different segments around the junction and whose input is the arrow display. The congestion prediction model relates the arrow display to the percentage of pedestrians that are

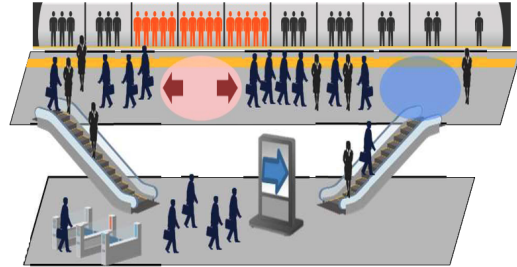


Fig. 1. Congestion balancing at train station. The predictive control technology guides pedestrians by means of an arrow display.

expected to change their intended walking direction upon seeing the arrow. Such parameters can be obtained by human factors experiments. The MPC formulation yields a mixed-integer quadratic program, which we solve with a computationally efficient relaxation. Further, this paper uses a quadratic convex optimization problem to estimate pedestrian flows from current and predicted congestion levels, which the MPC in turn uses for computing the arrow display. Finally, simulation results show that the proposed algorithm can significantly reduce congestion imbalance across different walkways and across different parts of a platform.

Related work

Related research areas in the literature are crowd management, mainly for safety and disaster prevention, see e.g., [1]–[16], and for vehicle traffic control, see e.g., [17]–[22].

Pedestrian Flow: Crowd control methods vary by their intended use and modeling techniques. In the following, we review some commonly investigated use-cases and models. In [1], a point-queue model within MPC is used for optimal pedestrian evacuation. In this point-queue model, pedestrian either traverse with free-flow velocity or queue with zero velocity. A comparative study of control strategies for emergency situations analyzing evacuation time is presented in [2]. In [3], the occupancies of the road network is balanced to reduce the risk of spillover of crowds in the roads. Further, [4] studies crowd control measures related to stampedes during large gatherings, and [5] presents a model for pedestrian flow using non-classical shocks. The works in [6]–[8] model movements using statistical moments, e.g., using leader-follower dynamics [6]. Leader-follower dynamics are also used within an MPC for crowd evacuation in [9]. The work in [10] studies self-ordered motion in systems of autonomous agents without a central planner. In [13], an evaluation index for safety of pedestrian is proposed, which considers congestion levels, [14] proposes a congestion evacuation model that includes panic behavior in a multi-agent framework, and [15] studies pedestrian evacuation guidance.

M. Menner and S. Di Cairano are with Mitsubishi Electric Research Laboratories (MERL), Cambridge, MA, 02139, USA (e-mail: menner@ieee.org, dicairano@ieee.org). M. Hamada and K. Gushima are with the Information Technology R&D Center, Mitsubishi Electric, Japan (e-mail: hamada.masaki@cw.mitsubishielectric.co.jp, gushima.kota@df.mitsubishielectric.co.jp).

Vehicle Flow: Both traffic signals and connected vehicles are used to regulate traffic flow, including mixed-traffic. In [17], autonomous vehicles are utilized to stabilize human-driven vehicles. Further, [18] studies smooth traffic flows at signaled intersections by decision tree policies based on imitating experts, and [19] uses reinforcement learning to minimize fuel consumption at intersections. In [20], a centralized route manager for autonomous vehicles is proposed for balancing traffic flows. In [21], a multi-agent control framework is proposed that decomposes a centralized MPC problem into a network of sub-problems, and [22] considers the control of automated vehicles by a central coordinator in mixed traffic with non-controlled vehicles.

II. CONGESTION AND PEDESTRIAN GUIDANCE MODEL

The following assumptions are made to derive a mathematical model for predicting congestion levels. First, upon seeing an arrow with maximum intensity, the percentage r [%] of pedestrians change their intended walking direction and choose the signaling segment. Next, upon seeing an arrow with reduced intensity $s \in [0, 100\%]$, the reduced percentage of pedestrians $r \cdot \rho(s)$ [%] are re-routed. Here, $\rho : [0, 100\%] \rightarrow [0, 100\%]$ with $\rho(0) = 0$ and $\rho(100\%) = 100\%$, and $\frac{\partial \rho(s)}{\partial s} > 0 \forall s$, i.e., monotonically increasing. Assuming ρ to be monotonically increasing is sensible as it implies that an arrow with higher intensity re-routes more pedestrians.

The following quantities are assumed to be available:

- The congestion levels at the current time, t ,
- congestion predictions at a future time, $t + N$, with no display action,
- the invertible mapping of re-routed pedestrians to arrow intensity, $r \cdot \rho(s)$.

This paper uses $r \cdot \rho(s) = r \cdot s$, i.e., the number of pedestrians being re-routed scales linearly with the intensity of the arrow. However, as ρ is invertible (due to monotonicity), a nonlinear ρ does not add complexity to the proposed algorithm. In practice, the map $r \cdot \rho(s)$ is not known exactly. Section V shows that the algorithm is robust to such an uncertainty.

A. Uncontrolled Congestion Model (Without Arrow Display)

Let $x_t^{\text{pre}} \in \mathbf{R}^{n_{\text{pre}}}$ be the number of pedestrians/the congestion level in the n_{pre} areas leading to the intersection at time t . Let $x_t^{\text{post}} \in \mathbf{R}^{n_{\text{post}}}$ be the congestion level in the n_{post} areas after the intersection. Further, let $x_t^{\text{pre},i} \in \mathbf{R}$ and $x_t^{\text{post},i} \in \mathbf{R}$ be the pedestrians in the respective i -th segment. We refer to the segments leading to the intersection as pre-segments and the segments after the intersection as post-segments. The time evolution of the congestion levels without guiding arrows are due to the pedestrians flows into and out of the segments,

$$\begin{bmatrix} x_{t+1}^{\text{pre}} \\ x_{t+1}^{\text{post}} \end{bmatrix} = \begin{bmatrix} x_t^{\text{pre}} \\ x_t^{\text{post}} \end{bmatrix} + \begin{bmatrix} \Delta x_{\text{in},t}^{\text{pre}} \\ \Delta x_{\text{in},t}^{\text{post}} \end{bmatrix} - \begin{bmatrix} \Delta x_{\text{out},t}^{\text{pre}} \\ \Delta x_{\text{out},t}^{\text{post}} \end{bmatrix}, \quad (1)$$

where $\Delta x_{\text{in},t}^{\text{pre}}$, $\Delta x_{\text{in},t}^{\text{post}}$, $\Delta x_{\text{out},t}^{\text{pre}}$, and $\Delta x_{\text{out},t}^{\text{post}}$ denote the pedestrian flows at time t into the pre-segments, into the post-segments, out of the pre-segments, and out of the post-segments, respectively, see Fig. 2 for an illustration. The

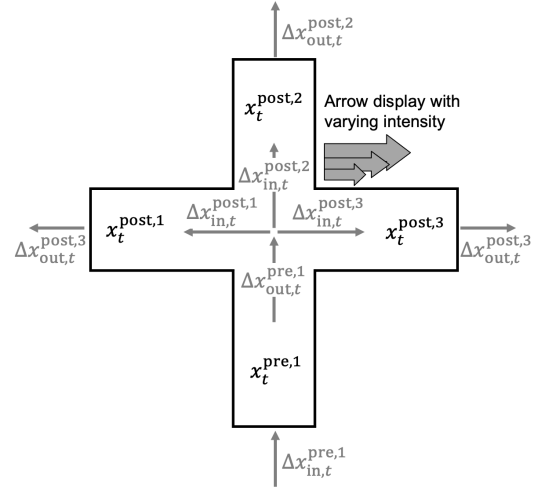


Fig. 2. Intersection scenario with three guidance directions, $n_{\text{post}} = 3$. The figure illustrates congestion levels, x_t , as well as pedestrian flows, Δx_t .

pedestrians entering the post-segments, $\Delta x_{\text{in},t}^{\text{post}}$, are the ones that see the arrow display and that may be re-routed.

B. Controlled Congestion Model (With Arrow Display)

For controlling congestion levels, we model the arrow display as input $u_t \in \mathbf{R}^{n_{\text{post}}}$, where u_t can have only one nonzero element, e.g., $u_t = [0, 0, 0.60]^T$ for $n_{\text{post}} = 3$ indicating an arrow of intensity 60% in the third segment. Hence compared to the congestion model in (1), the changes in the people flow controlled by means of an arrow are

$$\Delta x_{\text{in},t}^{\text{cl}} = r \begin{bmatrix} 0 \\ \bar{B}(\Delta x_{\text{in},t}^{\text{post}}) \end{bmatrix} u_t, \quad (2)$$

where $\bar{B}(\Delta x_{\text{in},t}^{\text{post}}) \in \mathbf{R}^{n_{\text{post}} \times n_{\text{post}}}$ is the *re-routing matrix*, whose element in the j th row and k th column is

$$\left[\bar{B}(\Delta x_{\text{in},t}^{\text{post}}) \right]_{jk} = \begin{cases} -\Delta x_{\text{in},t}^{\text{post},j} + \sum_{i=1}^{n_{\text{post}}} \Delta x_{\text{in},t}^{\text{post},i} & \text{if } j = k \\ -\Delta x_{\text{in},t}^{\text{post},j} & \text{else.} \end{cases}$$

For instance, for $n_{\text{post}} = 3$, there are three signaling direction,

$$\bar{B}(\Delta x_{\text{in},t}^{\text{post}}) = \begin{bmatrix} \Delta x^2 + \Delta x^3 & -\Delta x^1 & -\Delta x^1 \\ -\Delta x^2 & \Delta x^1 + \Delta x^3 & -\Delta x^2 \\ -\Delta x^3 & -\Delta x^3 & \Delta x^1 + \Delta x^2 \end{bmatrix}$$

where $\Delta x^i = \Delta x_{\text{in},t}^{\text{post},i}$, for shortness of the notation. The columns of $B(\Delta x_{\text{in},t}^{\text{post}})$ sum up to zero, which is due to pedestrian balance, e.g., when displaying an arrow in the direction of Segment 1, the percentage of pedestrians re-routed to Segment 1 is taken away from Segments 2 and 3.

Hence, the controlled congestion model is

$$\begin{bmatrix} x_{t+1}^{\text{pre}} \\ x_{t+1}^{\text{post}} \end{bmatrix} = \begin{bmatrix} x_t^{\text{pre}} \\ x_t^{\text{post}} \end{bmatrix} + \begin{bmatrix} \Delta x_{\text{in},t}^{\text{pre}} \\ \Delta x_{\text{in},t}^{\text{post}} \end{bmatrix} - \begin{bmatrix} \Delta x_{\text{out},t}^{\text{pre}} \\ \Delta x_{\text{out},t}^{\text{post}} \end{bmatrix} + r \begin{bmatrix} 0 \\ \bar{B}_t \end{bmatrix} u_t$$

with $\bar{B}_t := \bar{B}(\Delta x_{\text{in},t}^{\text{post}})$. To ease of notation, in the following we summarize the controlled congestion model as

$$x_{t+1} = x_t + \Delta x_{\text{in},t} - \Delta x_{\text{out},t} + r B_t u_t. \quad (3)$$

III. MPC FOR COMPUTING ARROW DISPLAY

A. Prediction model for MPC

The pedestrians that have been re-routed at time t will eventually leave the post-segments, i.e., the pedestrians contribute to the congestion levels only for a period of time. Let τ_t be the time that pedestrians stay in the post-segments. For a scenario in which the post-segments do not lead to a train platform, this time relates to the traversal time of the post-segment. In particular, the pedestrians entering post-segment i with length l at time t leave post-segment i at time $t+\tau_t$ with $\tau_t = l/v_{\text{ped}}$, on average. Different lengths of the post-segments, l_i , are straightforward to consider, which we omit for ease of notation. For a scenario in which the post-segments lead to a platform, τ_t relates to the time at which a train departs and to the time it takes to reach the platform. The difference between the two scenarios is that for the latter, pedestrians can only leave the post-segments whenever a train departs. In particular, the pedestrians entering post-segment i with length l at time t leave post-segment i at time $t+\tau_t$, where τ_t is the time of boarding the train. Note that $\tau_t \geq l/v_{\text{ped}}$, because the pedestrians need to traverse the post-segment in order to reach the platform before boarding a train. Using the average walking speed of pedestrians is suitable here as the main scope of this paper is balancing congestion at a macroscopic level. Hence, the MPC's congestion prediction model starting at time $t=0$ is

$$x_1 = x_0 + \Delta x_{\text{in},0} - \Delta x_{\text{out},0} + rB_0 u_0 \quad (4a)$$

$$x_2 = x_0 + \sum_{k=0}^1 (\Delta x_{\text{in},k} - \Delta x_{\text{out},k}) + \sum_{k=0}^1 rB_k u_k \quad (4b)$$

⋮

$$x_{N+1} = x_0 + \sum_{k=0}^N (\Delta x_{\text{in},k} - \Delta x_{\text{out},k}) + \sum_{k=t-\tau_N}^N rB_k u_k \quad (4c)$$

where τ_t is the time that the re-routed pedestrians stay in the post-segments.

B. Mixed-Integer and Input Constraints

The formulation in (3) is purposefully chosen to yield a linear and time-varying formulation, for a given control input, u_t . The displaying in one single direction imposes the constraint that only one element of u_t can be nonzero, which can be formulated as complementarity constraint $u_t^i u_t^j = 0$ for all $i \neq j$ or using auxiliary variables, δ_t^i , with

$$0 \leq u_t^i \leq 0 + \delta_t^i, \quad \delta_t^i \in \{0, 1\}, \quad \sum_{i=1}^{n_{\text{post}}} \delta_t^i = 1. \quad (5)$$

Finally, for many applications, it makes sense to have the algorithm not shift the arrow display too often. If the arrow display is to be kept constant for a time T_{shift} , then

$$u_t = u_{t+1} = \dots = u_{t+T_{\text{shift}}-1} \quad (6a)$$

$$u_{t+T_{\text{shift}}} = u_{t+T_{\text{shift}}+1} = \dots = u_{t+2T_{\text{shift}}-1} \quad (6b)$$

⋮

$$u_{t+n_{\text{shift}}T_{\text{shift}}} = u_{t+n_{\text{shift}}T_{\text{shift}}+1} = \dots = u_{t+N} \quad (6c)$$

with n_{shift} being the last shift in the MPC horizon.

C. MPC Formulations

Using the pedestrian congestion model (4), the mixed-integer constraint (5), the constraint for switching the display at certain times (6), and congestion target values x_{ref}^i , the optimal control problem is

$$\min_{u_t, \delta_t} \sum_{t=0}^N \sum_{i=1}^{n_{\text{post}}} \left(x_t^{\text{post},i} - x_{\text{ref}}^i \right)^2 \quad (7a)$$

$$\text{s.t.} \quad (4), (6), x_0 = x(t) \quad (7b)$$

$$(5) \quad \forall t. \quad (7c)$$

For applications with a long MPC prediction horizon, the MPC in (7) may become too computationally demanding. However, a useful alternative solution is to enforce the mixed integer constraint (7c) only for the first time step and use $0 \leq \sum_{i=1}^{n_{\text{post}}} u_t^i \leq 1$. Hence, the relaxed MPC is

$$\min_{u_t, \delta_0} \sum_{t=0}^N \sum_{i=1}^{n_{\text{post}}} \left(x_t^{\text{post},i} - x_{\text{ref}}^i \right)^2 \quad (8a)$$

$$\text{s.t.} \quad (4), (6), x_0 = x(t) \quad (8b)$$

$$(5) \quad t = 0 \quad (8c)$$

$$0 \leq \sum_{i=1}^{n_{\text{post}}} u_t^i \leq 1 \quad \forall t. \quad (8d)$$

The rationale for the relaxed problem (8) is exact for the near future and approximates the constraint along the rest of the prediction horizon. Eq. (8) can be optimized by solving n_{post} convex quadratic programs (one per post-segment) and choosing the solution with the smallest cost.

IV. PREDICTING PEDESTRIAN FLOWS

This paper considers a scenario in which only the current congestion at time t and the predicted congestion at $t+N$ are known. This section introduces a convex optimization problem to estimate the pedestrian flows, Δx , which the MPC uses as congestion prediction model (4). We separate the arrow display computation for given pedestrian flows and the pedestrian flow estimation for given congestion predictions, because it is computationally more efficient. This way, the MPC uses a linear time-varying prediction model and only a few integer variables, and the pedestrian flow estimation introduced in the following is convex.

A. Constraints and Cost for Predicting Pedestrian Flows

1) *Constraint for relating congestion levels with pedestrian flow for each individual segments:* This relates the changing congestion levels to the pedestrian inflow and outflow as in (1).

2) *Constraint for balancing pedestrian flow across intersection:* This accounts for the number of pedestrians passing the intersection, regardless of their decision of which segment to use,

$$\sum_{i=1}^{n_{\text{pre}}} \Delta x_{\text{out},t}^{\text{pre},i} = \sum_{i=1}^{n_{\text{post}}} \Delta x_{\text{in},t}^{\text{post},i}. \quad (9)$$

3) *Constraint for unidirectional flow:* This enforces the pedestrian flows to be positive, as illustrated in Fig. 2,

$$\Delta x_{\text{in}}^{\text{pre},i} \geq 0, \Delta x_{\text{out}}^{\text{pre},i} \geq 0 \quad \forall i = 1, \dots, n_{\text{pre}} \quad (10a)$$

$$\Delta x_{\text{in}}^{\text{post},i} \geq 0, \Delta x_{\text{out}}^{\text{post},i} \geq 0 \quad \forall i = 1, \dots, n_{\text{post}} \quad (10b)$$

4) *Constraint for train departure:* For a scenario with platform, the pedestrians can only leave the post-segments at the times that a train departs,

$$\Delta x_{\text{out},t}^{\text{post}} = 0 \quad \forall t \notin T_{\text{schedule}}, \quad (11)$$

where T_{schedule} is a set that includes all train departure times within the prediction horizon, N .

5) *Cost for average pedestrian walking speed:* This is related to how quickly pedestrians leave a segment after having entered the same segment, i.e., pedestrians entering pre-segment i at time t , leave the segment at time $t + \tau_i^{\text{pre}}$ and pedestrians entering post-segment i at time t , leave the segment at time $t + \tau_i^{\text{post}}$,

$$c_v^{\text{pre}} = \sum_{i=1}^{n_{\text{pre}}} \sum_{t=\tau_i^{\text{pre}}}^N (\Delta x_{\text{in},t-\tau_i^{\text{pre}}}^{\text{pre},i} - \Delta x_{\text{out},t}^{\text{pre},i})^2$$

$$c_v^{\text{post}} = \sum_{i=1}^{n_{\text{post}}} \sum_{t=\tau_i^{\text{post}}}^N (\Delta x_{\text{in},t-\tau_i^{\text{post}}}^{\text{post},i} - \Delta x_{\text{out},t}^{\text{post},i})^2,$$

where c_v^{post} is only relevant for a scenario with continuous pedestrian outflow of the post-segments.

6) *Cost for pedestrian accumulation on segments:* This cost relates the pedestrian flows to the congestion levels, i.e., the congestion level of a segment is a result of pedestrian inflows over a period of time related to the average walking speed, the segment's length, and the train schedule (if used at train stations). For the pre-segments,

$$c_a^{\text{pre}} = \sum_{i=1}^{n_{\text{pre}}} \sum_{t=\tau_i^{\text{pre}}}^N \left(x_t^{\text{pre},i} - \sum_{k=t-\tau_i^{\text{pre}}}^t \Delta x_{\text{in},k}^{\text{pre},i} \right)^2.$$

For a scenario with continuous outflow,

$$c_a^{\text{post}} = \sum_{i=1}^{n_{\text{post}}} \sum_{t=\tau_i^{\text{post}}}^N \left(x_t^{\text{post},i} - \sum_{k=t-\tau_i^{\text{post}}}^t \Delta x_{\text{in},k}^{\text{post},i} \right)^2.$$

For a scenario leading to a platform in a train station,

$$c_{\text{train}}^{\text{post}} = \sum_{i=1}^{n_{\text{post}}} \sum_{t=1}^N \left(x_t^{\text{post},i} - \left(x_{\tau_t}^{\text{post},i} + \sum_{k=\tau_t}^t \Delta x_{\text{in},k}^{\text{post},i} \right) \right)^2$$

where $\tau_t \geq 0$ is the time of departure of the train prior to time t . For example, let there be one train at $t = 5$. Then, $\tau_0 = \tau_1 = \dots = \tau_4 = 0$ and $\tau_5 = \dots = \tau_N = 5$.

B. Optimization for Estimating Pedestrian Flows

Here, we combine all elements introduced in Section IV-A to state the convex optimization problems for the two scenarios. For a scenario with continuous outflow,

$$\min_{\Delta x, x} c_v^{\text{pre}} + c_v^{\text{post}} + c_a^{\text{pre}} + c_a^{\text{post}} \quad (12a)$$

$$\text{s.t.} \quad (1), (9), (10) \quad (12b)$$

$$x_0 = x(t) \quad \text{current congestion} \quad (12c)$$

$$x_N = x(t + N) \quad \text{predicted congestion.} \quad (12d)$$

For the scenario at a train station,

$$\min_{\Delta x, x} c_v^{\text{pre}} + c_a^{\text{pre}} + c_{\text{train}}^{\text{post}} \quad (13a)$$

$$\text{s.t.} \quad (1), (9), (10) \quad (13b)$$

$$(11) \text{ if train schedule available} \quad (13c)$$

$$x_0 = x(t) \quad \text{current congestion} \quad (13d)$$

$$x_N = x(t + N) \quad \text{predicted congestion.} \quad (13e)$$

V. SIMULATION RESULTS

A. Simulation Setup

We consider a scenario with one pre-segment, $n_{\text{pre}} = 1$, and three post-segment, $n_{\text{post}} = 3$, with lengths $l = 200\text{m}$. We assume an average pedestrian walking speed of $v_{\text{ped}} = 1\text{m/s}$, i.e., pedestrians need $l/v_{\text{ped}} = 200\text{s}$ to traverse the post-segments. We use a sampling time step of $T_s = 0.5\text{min}$ and an MPC horizon of 10min , i.e., $N = 20$. We enforce the arrow-shifting constraint in (6) to allow changes every 2min . We assume $r = 0.5$, i.e., 50% of pedestrians change their walking direction after seeing an arrow with maximum intensity. We use the relaxed MPC in (8) due to its ease of implementation. Using the non-relaxed MPC in (7) may increase accuracy further. We compute the congestion imbalance at time t as $\frac{1}{3}(|x_t^{\text{post},1} - x_t^{\text{post},2}| + |x_t^{\text{post},1} - x_t^{\text{post},3}| + |x_t^{\text{post},2} - x_t^{\text{post},3}|)$.

We present Monte Carlo simulation trials of a scenario lasting 140min . For each trial, the pedestrian flows are sampled from two sets of uniform distributions. First, we sample values from the uniform distribution $\mathcal{U}(5, 20)$, where each value correspond to a mean pedestrian flow in each post-segment for a 30min window. Second, we sample values from the uniform distribution $\mathcal{U}(-1, 1)$ at each time representing noise. Hence, $\Delta x_{\text{in}}^{\text{post},i} = \tilde{x}_{\text{mean}} + \tilde{x}_{\text{noise}}$ with $\tilde{x}_{\text{mean}} \sim \mathcal{U}(5, 20)$ and $\tilde{x}_{\text{noise}} \sim \mathcal{U}(-1, 1)$ for all post-segments i . The flows in the pre-segments and outflows out of the post-segments are chosen to match the constraints in Section IV. The constant mean pedestrian flow for a 30min period is not necessary, but chosen to facilitate easy explanation and interpretation of the figures in this section. We study three scenarios, which are laid out in the following.

1) *No train platform:* In the first scenario, the post-segments do not lead up to a train platform. Hence, the pedestrians do not leave the post-segments at any time.

2) *Train platform but unknown train schedule:* In the second scenario, the post-segments lead to a train platform. A train departs every 10min . However, here we consider that the train schedule is not known. We study this scenario as it illustrates how the algorithm can cope with uncertainty in the train schedule. We implement a constraint that no pedestrians can leave the post-segments within the MPC horizon. Hence, a train leaving the station is treated as a disturbance.

3) *Train platform and known train schedule:* In the third scenario, the post-segments lead to a train platform, and where the train schedule is given. Hence, the algorithm leverages the information about the times when pedestrians can leave the post-segments on a train. Here, too, trains depart in 10min intervals.

B. Illustration and Interpretation of Results

Fig. 3 illustrates one simulation trial. It shows both congestion levels that would have resulted had no arrow display been shown and congestion levels where pedestrians are guided. Fig. 3 illustrates Scenario 1 in Section V-A.1 with continuous pedestrian outflow, i.e., no platform. Fig. 3 presents a simulation trial in which pedestrians favor the blue post-segment, see top plot. Consequently, the algorithm displays an arrow to guide the pedestrians away from the blue

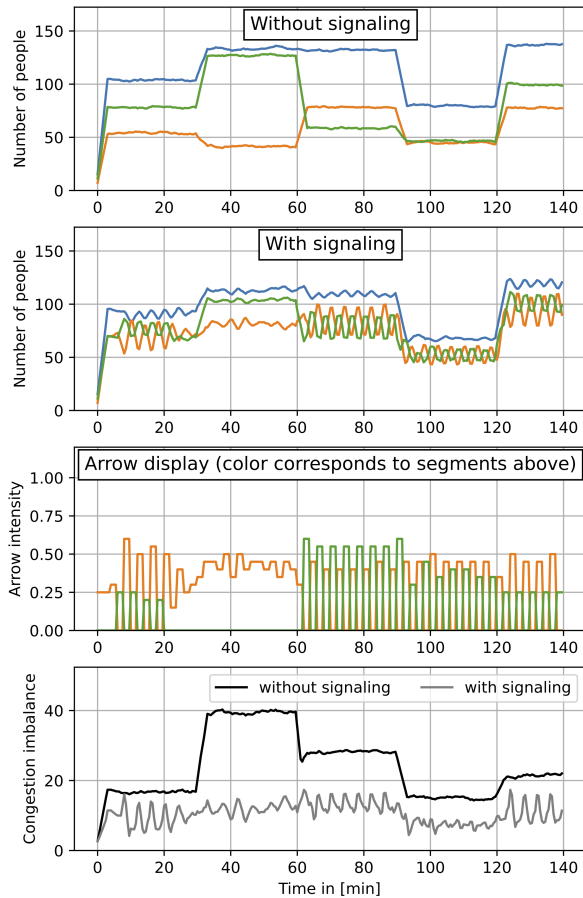


Fig. 3. Congestion imbalance of three post-segments without and with arrow display. Top: Congestion imbalance without display. Second from top: Congestion imbalance with display. Third from top: Arrow display computed with presented technology. Bottom: Congestion imbalance. The plots illustrate the benefits of using an arrow display computed by model predictive control to balance congestion.

post-segment into the orange and green post-segments. The MPC alternates between the two less traveled post-segments as the MPC cannot show an arrow in two directions. The predictive nature of the proposed algorithm can be seen best in the third plot in Fig. 3 during the interval 20–30min. Here, the arrow display stops signaling into the green post-segment anticipating that more pedestrians will be traversing the green post-segment during the interval 30–60min. The qualitative results after guidance in the second plot from the top show that congestion levels are significantly closer, which can also be seen in the congestion imbalance plot. In this trial, the congestion imbalance has been reduced by 56% on average.

Fig. 4 illustrates Scenario 3 in Section V-A.3 with a train platform. Scenario 2 in Section V-A.2 is not illustrated as it yields similar graphs to Fig. 4. The train departures can be identified by sudden drops in pedestrians on the platform. In the illustrated scenario, the orange post-segment is traversed less frequently during the intervals 0–30min and 90–120min in the top plot. Hence, the MPC displays an arrow with appropriate intensity to balance congestion, see the same intervals in the third plot. Consequently, pedestrians are re-routed into the orange post-segment reducing the congestion

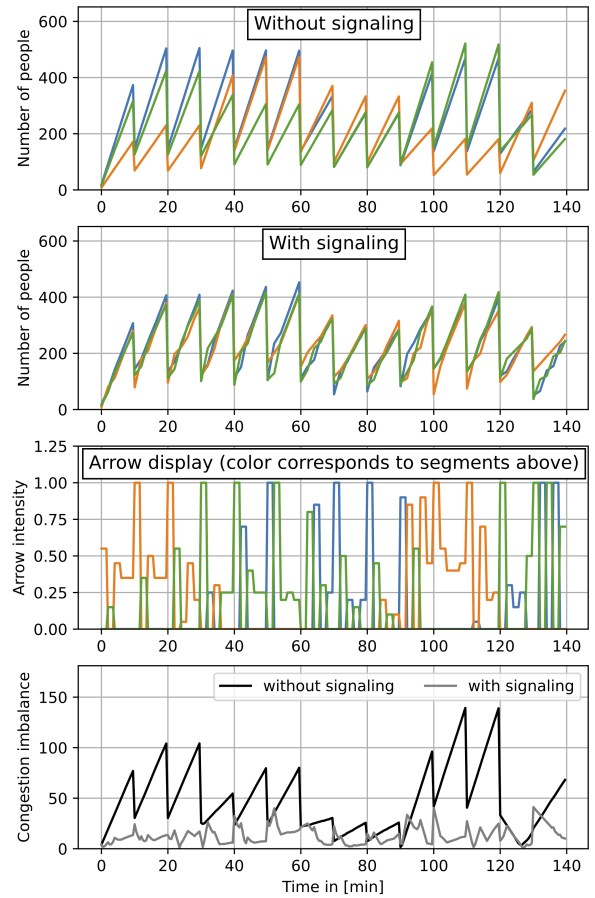


Fig. 4. Congestion imbalance of three post-segments at train station without and with arrow display. Top: Congestion imbalance without arrow. Second from top: Congestion imbalance with arrow. Third from top: Arrow display computed with presented technology. Bottom: Congestion imbalance.

imbalance significantly. The reduced congestion imbalance is illustrated in the bottom plot. The congestion imbalance reduction in the simulation trial displayed in Fig. 4 is 76%.

C. Statistical Evaluation

Fig. 5 shows statistics of 500 Monte Carlo trials of the setup in Section V-A. For Scenario 1 with continuous people outflow, congestion imbalance is reduced by 47%–62% with a median of 54%. For Scenario 2, the congestion imbalance is reduced by 29%–58% with a median of 49%. This scenario exhibits the largest spread as the train schedule is not included in the algorithm. For Scenario 3, the congestion imbalance reduction can be expected to be superior to Scenario 2 as more information is used. Here, the congestion imbalance is reduced by 61%–76% with a median of 70%.

Table I shows median congestion imbalance reductions for variations of the three scenarios in Fig. 5. First, Table I shows how much the congestion imbalance is reduced when the pedestrian flows are given (rather than estimated). Consequently, the imbalance can be reduced more as the pedestrian flows are more accurate. However, using a train schedule, the pedestrian flows are recovered quite accurately as the congestion imbalance reductions are similar for given and estimated flows, which is due to the train-departure

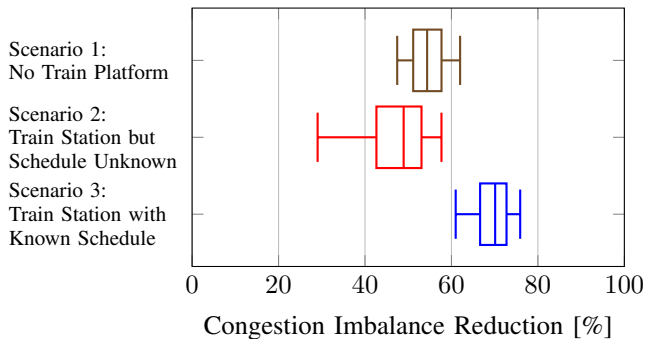


Fig. 5. Statistics of 500 Monte Carlo trials. The plot shows congestion imbalance reduction when using the arrow display. It shows box-plots for all three scenarios representing the 10th percentile, the 25th percentile, the 50th percentile (the median), the 75th percentile, and the 90th percentile.

TABLE I
EXTENDED STUDY OF IMBALANCE REDUCTION

Scenario	Schedule	Flows	Arrow	Imbalance Reduction
train	known	estimated	varying unit	70% (in Fig. 5)
train	known	estimated	unit	63%
train	known	given	varying unit	76%
train	known	given	unit	63%
train	unknown	estimated	varying unit	49% (in Fig. 5)
train	unknown	estimated	unit	48%
train	unknown	given	varying unit	74%
train	unknown	given	unit	61%
no train	N/A	estimated	varying unit	54% (in Fig. 5)
no train	N/A	estimated	unit	9%
no train	N/A	given	varying unit	64%
no train	N/A	given	unit	17%

constraints. Second, Table I shows simulation results where the intensity of the arrow display cannot be used as a degree of freedom. Here, the MPC can either choose to not display an arrow or to display a unit arrow in one of the three segments. As expected, the congestion imbalance is reduced less due to removing the degree of freedom of a varying intensity. Finally, we have conducted a robustness simulation study, where at each simulation trial we sampled $r_{\text{true}} \in [30\%, 70\%]$ and the MPC used $r = 50\%$. Here, for Scenario 1, the median congestion imbalance reduction is 68%; for Scenario 2, 48%; and for Scenario 3, 53%. This robustness evaluation indicates the applicability of the algorithm in practice, where r may only be known approximately from human factor studies and experimental data.

VI. CONCLUSIONS

This paper presented an MPC-based algorithm for routing pedestrians in crowded places in order to balance congestion levels. The pedestrian guidance algorithm used a convex optimization problem to estimate pedestrian flows from congestion predictions and a mixed-integer program with only a few mixed-integer constraints to compute an arrow display for balancing congestions. Simulation results show that the algorithm was able to reduce congestions at train stations between 61%–76% with a median of 70%, and in scenarios with a continuous outflow between 47%–62% with a median of 54%. Further, robustness studies with respect to modeling uncertainty indicate the algorithm’s applicability in practice.

REFERENCES

- [1] O. B. Västberg, H. Dong, and X. Hu, “Optimal pedestrian evacuation using model predictive control,” in *2013 European Control Conference (ECC)*, pp. 1224–1229, 2013.
- [2] C. Pacheco, P. Karelavic, and A. Cipriano, “Comparing dynamic evacuation control strategies for emergency situations,” in *2015 European Control Conference (ECC)*, pp. 3053–3058, 2015.
- [3] R. Gao, A. Zha, S. Shigenaka, and M. Onishi, “Hybrid modeling and predictive control of large-scale crowd movement in road network,” in *Proceedings of the 24th International Conference on Hybrid Systems: Computation and Control*, pp. 1–7, 2021.
- [4] Y. A. Alaska, A. D. Aldawas, N. A. Aljerian, Z. A. Memish, and S. Suner, “The impact of crowd control measures on the occurrence of stampedes during mass gatherings: The Hajj experience,” *Travel medicine and infectious disease*, vol. 15, pp. 67–70, 2017.
- [5] R. M. Colombo and M. D. Rosini, “Pedestrian flows and non-classical shocks,” *Mathematical methods in the applied sciences*, vol. 28, no. 13, pp. 1553–1567, 2005.
- [6] Y. Yang, D. V. Dimarogonas, and X. Hu, “Shaping up crowd of agents through controlling their statistical moments,” in *2015 European Control Conference (ECC)*, pp. 1017–1022, 2015.
- [7] S. Zhang, A. Ringh, X. Hu, and J. Karlsson, “A moment-based approach to modeling collective behaviors,” in *2018 IEEE Conference on Decision and Control (CDC)*, pp. 1681–1687, 2018.
- [8] S. Zhang, A. Ringh, X. Hu, and J. Karlsson, “Modeling collective behaviors: A moment-based approach,” *IEEE Transactions on Automatic Control*, vol. 66, no. 1, pp. 33–48, 2020.
- [9] J. Tianhe and S. Ziheng, “Optimal control on crowd evacuation with leader-follower model,” in *2018 11th International Symposium on Computational Intelligence and Design*, vol. 2, pp. 236–239, 2018.
- [10] T. Vicsek, A. Czirók, E. Ben-Jacob, I. Cohen, and O. Shochet, “Novel type of phase transition in a system of self-driven particles,” *Physical review letters*, vol. 75, no. 6, p. 1226, 1995.
- [11] A. Jadbabaie, J. Lin, and A. S. Morse, “Coordination of groups of mobile autonomous agents using nearest neighbor rules,” *IEEE Transactions on Automatic Control*, vol. 48, no. 6, pp. 988–1001, 2003.
- [12] R. Olfati-Saber, “Flocking for multi-agent dynamic systems: Algorithms and theory,” *IEEE Transactions on Automatic Control*, vol. 51, no. 3, pp. 401–420, 2006.
- [13] S. Shigenaka, S. Takami, Y. Ozaki, M. Onishi, T. Yamashita, and I. Noda, “Evaluation of optimization for pedestrian route guidance in real-world crowded scene,” in *AAMAS*, pp. 2192–2194, 2019.
- [14] J. Wang, L. Zhang, Q. Shi, P. Yang, and X. Hu, “Modeling and simulating for congestion pedestrian evacuation with panic,” *Physica A: Statistical Mechanics and its Applications*, vol. 428, pp. 396–409, 2015.
- [15] J. C. Chu, A. Y. Chen, and Y.-F. Lin, “Variable guidance for pedestrian evacuation considering congestion, hazard, and compliance behavior,” *Transportation Research Part C: Emerging Technologies*, vol. 85, pp. 664–683, 2017.
- [16] C. Martella, J. Li, C. Conrado, and A. Vermeeren, “On current crowd management practices and the need for increased situation awareness, prediction, and intervention,” *Safety science*, vol. 91, pp. 381–393, 2017.
- [17] C. Wu, A. M. Bayen, and A. Mehta, “Stabilizing traffic with autonomous vehicles,” in *2018 IEEE international conference on robotics and automation (ICRA)*, pp. 6012–6018, 2018.
- [18] V. Jayawardana, A. Landler, and C. Wu, “Mixed autonomous supervision in traffic signal control,” in *2021 IEEE International Intelligent Transportation Systems Conference (ITSC)*, pp. 1767–1773, 2021.
- [19] V. Jayawardana and C. Wu, “Learning eco-driving strategies at signalized intersections,” in *2022 European Control Conference (ECC)*, pp. 383–390, 2022.
- [20] J. L. Zambrano-Martinez, C. T. Calafate, D. Soler, L.-G. Lemus-Zúñiga, J.-C. Cano, P. Manzoni, and T. Gayraud, “A centralized route-management solution for autonomous vehicles in urban areas,” *Electronics*, vol. 8, no. 7, p. 722, 2019.
- [21] L. B. De Oliveira and E. Camponogara, “Multi-agent model predictive control of signaling split in urban traffic networks,” *Transportation Research Part C: Emerging Technologies*, vol. 18, no. 1, pp. 120–139, 2010.
- [22] R. Firoozi, R. Quirynen, and S. Di Cairano, “Coordination of autonomous vehicles and dynamic traffic rules in mixed automated/manual traffic,” in *2022 American Control Conference (ACC)*, pp. 1030–1035, 2022.